Makara Journal of Science

Volume 26
Issue 2 *June*

Article 8

6-30-2022

Silver Nanoparticles' Biosynthesis and Characterization with the Extract of Jatropha curcas Leaf: Analysis of Corrosion Inhibition Activity

Talabi Henry Kayode
Department of Metallurgical and Materials Engineering, Federal University of Technology, Akure 5664, Nigeria, hktalabi@futa.edu.ng

Talabi Justina Yetunde
Department of Human Nutrition and Dietetics, Afe Babalola University, Ado-Ekiti 360001, Nigeria

Adewuyi Benjamin Omotayo
Department of Metallurgical and Materials Engineering, Federal University of Technology, Akure 5664, Nigeria

Makara Journal of Science, 26/2 (2022), 137–144
doi: 10.7454/mss.v26i2.1276

Silver Nanoparticles' Biosynthesis and Characterization with the Extract of *Jatropha curcas* Leaf: Analysis of Corrosion Inhibition Activity

Talabi Henry Kayode[1*], Talabi Justina Yetunde[2], and Adewuyi Benjamin Omotayo[1]

1. Department of Metallurgical and Materials Engineering, Federal University of Technology, Akure 5664, Nigeria
2. Department of Human Nutrition and Dietetics, Afe Babalola University, Ado-Ekiti 360001, Nigeria

[*]*E-mail: hktalabi@futa.edu.ng*

Received August 31, 2021 | Accepted June 30, 2022

Abstract

The plant-mediated nanoparticles synthesis process is gaining popularity because of its effective cost, eco-friendliness, and nontoxic nature. The current study presents the silver nanoparticles (AgNPs) which synthesized with $AgNO_3$ as precursor salt and *Jatropha curcas* leaf extract. J. *curcas* leaf extract has phytochemicals that could reduce the precursor metal salt to nanoparticles and act as a capping agent surround the nanoparticles to enhance its stability. Phytochemical screening on J. curcas leaf extract showed that alkaloids, saponins, tannins, flavanoids, steroids, philobatannins, phenols, and cardiac glycosides are contained in the sample. The biosynthesized nanoparticles were investigated by UV-visible (UV-vis) spectroscopy, X-ray diffraction (XRD), and Fourier transform infrared spectroscopy (FTIR). UV-vis spectroscopy confirmed the fabrication of AgNPs at 250–400 nm. The solutions' change of color from pale yellow to reddish brown indicated that AgNPs is formed. XRD analysis revealed that the synthesized AgNPs average crystal size was 36.4 nm. FTIR analysis indicated that the organic residues covered the nanoparticles. The inhibitory properties of the solution of the synthesized nanoparticles and the bulk extract were evaluated using medium carbon steel. The solution of the synthesized nanoparticles (10 ml) showed better corrosion inhibition efficiency of 87.10 % compared with the bulk extract.

Keywords: fourier transform infrared, nanoparticles, synthesis, corrosion inhibition, X-ray diffraction

Introduction

Plants have received great attention because their typical elements have diverse usages in research and development [1]. Plant extracts contain a variety of natural chemical substances, which are usually called natural products. These natural substances have different biological characteristics due to the extraordinary variation in its chemical structures. The phytomolecules in plants extract allow the synthesis of nanoparticles (NPs) by functioning as the reductor [2] and promoting the process under controlled pressure and temperature. Plant extracts could be applied for the synthesis of NPs that are directly accessible for a number of applications, especially biological and catalytic usages [3].

Jatropha curcas is viewed as a weed or tree contributing to the bushy environment in Sub-Saharan Africa and Nigeria. It self-propagates in areas that have not been fully colonized. *J. curcas* is conventionally applied for the treatment of bacterial and fungal infections, febrile diseases, muscle pain, or jaundice treatments [4]. Among the energy crops of first-generation biofuels, *J. curcas* is an encouraging candidate [5].

Plant-facilitated metallic NP (MNP) synthesis is an evolving technique for the green synthesis of NPs and has different uses in industrial fields. MNP biocompatibility is mostly accredited to the phytochemicals in plant that cap surround the NPs to lessen its toxic property and enhance its stability [6]. NPs that are chemically prepared normally leave unreacted reductors, mostly toxic residue, on surfaces; therefore, phytochemicals are applied to make the NPs nontoxic [7]. Compared with that assisted by microorganisms, NP biosynthesis with plant extract is quick, stable, and has more advantages because it removes the cell culture preservation and could be scaled up easily [8].

Many researchers worldwide are trying new synthesis methods for diverse materials at the nanoscale to improve the materials' properties [9]. Research, development, and industrial activities have grown rapidly in the area of nanotechnology for the past decade [10, 11]. In general, NPs are particles having diameters in the range of 1–100 nm [12]. In the context of biotechnology, NPs have

diameters of up to 500 nm [13]. Different physical and chemical process can be applied to synthesize the nanomaterials. However, existing procedures are tremendously costly [14] and require toxic, hazardous chemicals called stabilizers, which might cause great risk environmentally and biologically. The following plants extracts are commonly applied for the synthesis of AgNPs with antimicrobial activities: leaf extracts of *Tridax procumbens*[15], *Moringa oleifera leaf* [16], *Lysiloma acapulcensis* [17], *Xanthium strumerium L*. [18], and *Murraya koenigii* (curry leaf) [19]. In this study, the phytocompounds in the plants extract acted as reducing and capping agents in the reaction with $AgNO_3$, a common applied precursor in silver nanoparticle (AgNP) synthesis.

The AgNPs synthesis from plants extracts is earth-friendly, reduces energy consumption, as well as can be performed at a large scale. AgNPs can act as anticorrosion agent to form protection layer on the metal surface. For example, Ituen et al[20] studied the impact of green synthesis and anticorrosion activity of *Allium cepa* peel extract- AgNP (Et-AgNP) composite on the simulation of the oilfield pickling solution and found that compared with the crude extract, Et-AgNPs were more effective and thermally stable as another option for the earth-friendly anticorrosion auxiliary for cleaning and pickling agent in industry. In this study, AgNPs were prepared with the leaf extracts of *J. curcas*, and their corrosion inhibitory efficiency on carbon steel in chloride environment was examined.

Materials and Methods

J. curcas leaves (Figure 1) were obtained from Akure, Nigeria (N 7° 15' 25.6788", E 5° 12' 20.8476"), sundried, and pulverized separately with a pulverizer with model number ES-1731F, power of 300 W, frequency of 50 Hz, and an AC voltage of 220 V. In brief, 10 g of the pulverized *J. curcas* leaves were weighed, soaked in 200 ml of distilled water, and refluxed in a water bath. Then, the compound was refined to obtain *J. curcas* leaf extracts [2, 20].

Phytochemical analysis of *J. curcas* plant extract. The phytochemicals from plants were determine using a standard method [21].

Biosynthesis of AgNPs. In brief, 0. 1 M $AgNO_3$ solution was mixed with *J. curcas* leaf aqueous extract at a ratio of 1:1 (v/v) to a volume of 50 ml in a flask. The obtained mixture was heated under microwave irradiation at a power of 300 W for 10 minutes [22] for complete bioreduction, and the color change was monitored with the naked eye.

Characterization of AgNPs

UV-visible (UV-vis) spectra of AgNPs. UV-vis spectroscopy is among the common methods applied to characterize the structure of NPs. The absorbance spectrum of green-synthesized AgNPs was analyzed using UV-vis spectroscopy [UV-vis spectrophotometer UV-2450 (Shimadzu)].

X-ray diffraction (XRD) analysis. The XRD analysis of synthesized AgNPs was conducted on a Shimadzu XRD-6000/6100 model with 30 kV, 30 mA with Cukα radian at angle 2θ. The nanocrystals' mean size was determined from the diffraction peaks broadening corresponded to the highest intensive reflections in accordance with the International Centre for Diffraction Data database. Scherrer equation [23] (equation [1]) was applied to define the crystallite size from the XRD diffraction pattern of NPs, where K is the Scherrer constant (shape factor, its value is 0.9), λ is the X-ray wavelength (λ = 0.154 nm), B is the line broadening at half the maximum intensity (FWHM) in radian:

$$d = \frac{K\lambda}{B\ cos\theta}. \quad (1)$$

Fourier transform infrared (FT-IR) spectroscopy. The obtained centrifuged and redispersed AgNPs were dried into powder, and the purified suspension was lyophilized. The resulting lyophilized powder was studied by infrared (IR) spectra registered on a Bruker Vector-22 infrared spectrophotometer using KBr pellets.

Corrosion studies. The AgNPs synthesized from *J. curcas* were tested for their corrosion inhibitory properties on medium carbon steel in seawater by electrochemical technique. The steel was cut into samples of 10 mm by 20 mm dimension. The chemical composition of the steel is displayed in Table 1. The samples were polished to remove dirt, scales and rust, and the surface

Figure 1. *Jatropha curcas* Plant

Table 1. The Medium Carbon Steel's Chemical Compositions

Element	Fe	C	P	Mn	Cr	Ni	S	Si	Al	Mo
Weight (%)	97.671	0.358	0.053	0.851	0.140	0.139	0.056	0.286	0.042	0.017

was treated with ethanol. The coupons were immersed in the corrosive medium containing a mixture of the environment, varying concentrations of AgNP solution, and plant extract. The corrosion behaviors of the samples were monitored, and the inhibition efficiency was measured with the equation 2 [24]:

$$I.E = \frac{\text{CRblank}-\text{CRinh}}{\text{CRblank}} \text{ x } 100\% \text{ ,} \qquad (2)$$

where I.E is the inhibiting efficiency, CR_{blank} is the corrosion rate in the absence of inhibitor, and CR_{inh} is the corrosion rate with inhibitor [24].

The chemical composition of the medium carbon steel was determined using spark spectrometric analysis and is presented in Table 1.

Results and Discussions

Phytochemical screening of *J. curcas* leaf aqueous extract. The alkaloids, saponins, tannins, flavanoids, steroids, philobatannins, phenols, and cardiac glycosides in the extract were screened using several qualitative tests as presented in Table 2.

Visual examination. As shown in Figure 2, the light yellow color changed to muddy after the silver nitrates was added to the *J. curcas* leaf extract. The mixture was kept under microwave irradiation, and the color transformation from muddy to dark brown affirmed that the AgNP has been formed. The dark brown color was a sign that the aqueous silver ions in the reaction mixture were reduced to silver nitrates [25] and was generated because the surface plasmon resonance (SPR) excitation of the AgNPs [26, 27]. The free electrons of AgNPs gave rise to SPR absorbance as a result of the combination of electrons vibration of the MNPs in resonance with the light waves [20].

UV-vis spectra. SPR analysis was applied to investigate the formation and stability of AgNP in the solution using UV-vis spectrophotometry. The bandwidth and shift variations in resonance can be used as parameters to characterize the formed AgNPs. Figure 3 presents the UV-vis absorption spectra of the AgNPs prepared using *J. curcas* leaf extract. Numerous absorption peaks were observed in 200–260 nm for the leaf extract. For the AgNPs, the peaks were in the range of 250–400 nm that was related to the SPR of AgNPs [28].

XRD. The crystal structure and size of NPs were analyzed using XRD. Figure 4 shows the XRD pattern for the AgNPs synthesized using *J. curcas* leaf extract. Four characteristic diffraction peaks at 32.6°, 44.3°, 60.2°, and 73.6° were found in the 2θ range and conformed to (111), (200), (220), and (311) planes, respectively. This finding indicated that the resultant NPs had a face-centered cube structure. On the basis of the XRD patterns, the NPs were presumed to be established by the reduction of Ag^+ ions by phytochemicals of *J. curcas* leaf extract. In addition, the NPs were crystalline in nature. Several supplemental and unknown peaks were also observed in the vicinity of the characteristic peaks of NPs and were linked to the presence of some bioorganic compounds in the extract. According to Scherrer equation, the average crystallite size of the synthesized AgNPs was 36.4 nm [29].

Table 2. Phytochemical Screening of *J. curcas* Leaf Aqueous Extract

S/N	Phytochemical	Qualitative
1	Alkaloids	+
2	Saponins	+
3	Tannins	+
4	Flavonoids	+
5	Steroids	+
6	Philobatannins	+
7	Phenols	+
8	Cardiac glycosides	+

Figure 2. Pictorial Representation of the Synthesis of the Nanomaterials Showing the Colors of the Reactants and the Product [2]

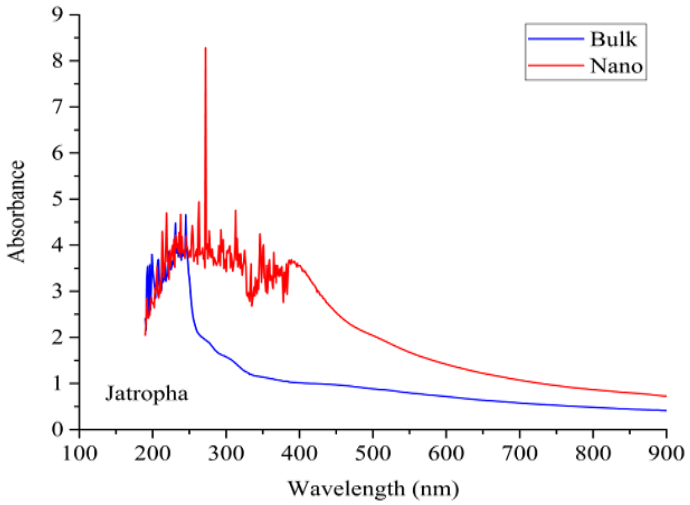

Figure 3. UV-vis Absorption Spectra of *J. curcas* Leaf Extract and *J. curcas* Synthesized Silver Nanoparticle Solution [2]

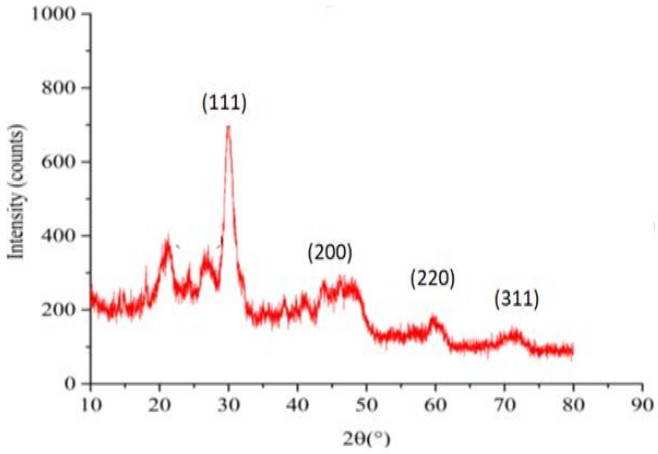

Figure 4. X-ray Diffraction Pattern of the Synthesized Silver Nanoparticles from *J. curcas* Leaf Extract

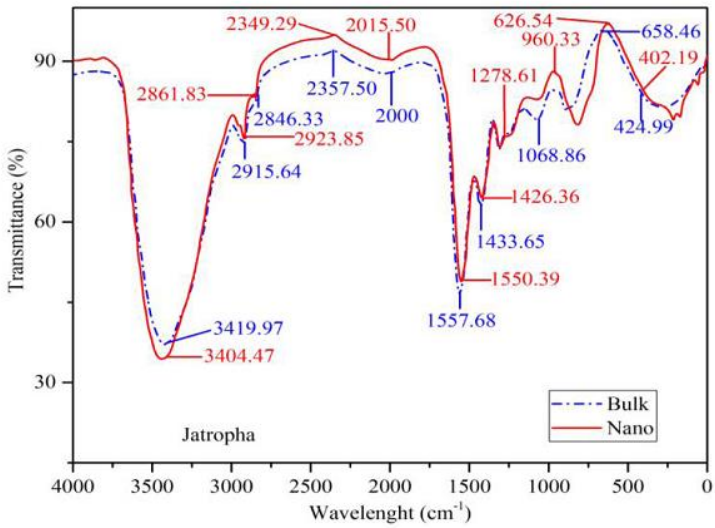

Figure 5. Fourier Transform Infrared Spectroscopy Spectra of *Jatropha curcas* Extract

Table 3. Potentiodynamic Polarization of *J. curcas* Extracts in Sea Water

Extract (*Jatropha curcas*)	Vol (ml)	E corr	βa	βc	I_{corr} ($\mu A.cm^{-2}$)	IE (%)
			(mV.decade)			
Control	0.0	−618.272	81.818	361.180	50.603	-
Bulk	7.5	−609.344	91.482	339.408	49.612	1.96
	10	−609.75	101.345	248.548	45.412	10.26
Nano	7.5	−575.122	128.347	252.362	37.71	25.48
	10	−454.177	30.425	204.585	6.53	87.10

FTIR analysis. FTIR spectroscopy was employed for the characterization and identification of the biomolecules of *J. curcas* leaf extract. The FTIR absorption spectra of *J. curcas* leaf extract before and after bioreduction are presented in Figure 5. The main absorbance bands in the spectrum of *J. curcas* leaf extract were found at 3419, 2915, 2846, 1557, and 1433 cm^{-1}. The broadband appeared at 3419 cm^{-1} can be attributed to the stretching vibrations of O–H groups in the leaf extract [30]. The bands at 2915 and 2846 conformed to the stretching vibrations of CH group [31]. The sharp peak at 1557 and 1433 can be attributed to carbonyl group [32]. The spectrum of the reduced *J. curcas* leaf extract showed characteristic absorbance bands at 3404, 2923, 2861, 2349, 2015, 1550, and 1426 cm^{-1}. In the IR spectrum of NP, the shifts of band peaks from 3419 cm^{-1} to 3404 cm^{-1}, 2915 cm^{-1} to 2923 cm^{-1}, and 1557 cm^{-1} to 1550 cm^{-1} corresponded to OH, CH, and carbonyl group, respectively, with low band intensity. Therefore, the hydroxyl and carbonyl groups of *J. curcas* leaf extract were taken part in the synthesis of AgNPs [33].

Corrosion studies. The curves of potentiodynamic polarization for the corrosion characteristic of the medium carbon steel in sea water without and with different concentrations of *J. curcas* leaf extract (bulk) and its nanostructure with AgNPs (nano) are displayed in Figure 6 and Table 3. The cathodic and anodic current densities (I_{corr}) decreased remarkably upon the introduction of *J. curcas* leaf extract (bulk) and its nanostructure with AgNPs (nano) in the sea water. The same trend was observed for the corrosion potential (E_{corr}) in the presence of bulk and nano, that is, a shift towards the negative direction in contrast to the blank solution. Table 3 shows that compared with that of the blank solution, I_{corr} decreased in the presence of *J. curcas* leaf extract (bulk) and its nanostructure with AgNPs (nano) and further decreased when the concentration of bulk and nano increased. In particular, the NP showed better corrosion inhibition property than the bulk. This finding suggested that *J. curcas* leaf extract (bulk) and its nanostructure with AgNPs (nano) inhibited the acid-induced corrosion of medium carbon

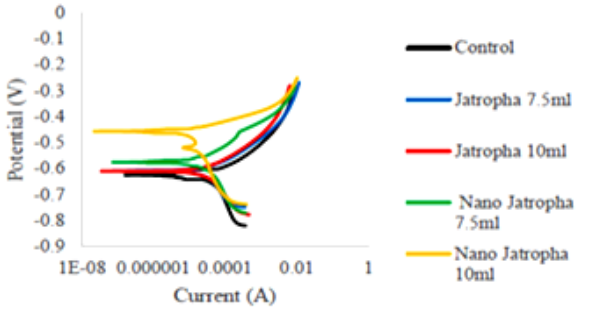

Figure 6. Tafel Plot of Coupon Immersed in Seawater Containing Different Volumes of *J. curcas* Extracts

steel. Table 3 also show some transformation in the anodic and cathodic Tafel slopes. The presence of the inhibitors (bulk and nano) led to a reduction in the corrosion rate. Meanwhile, the inhibition efficiency (IE) enhanced by the *J. curcas* leaf extracts concentration and nanostructure AgNP solution. The enhance in IE might be the result of a protective film formation assigned to the metal/solution interface transition from an active dissolution state to a passive state.In addition,the solution of the synthesized AgNPs (10 mL) showed better corrosion IE of 87.10% than the bulk. Although the NP solution reduced the dissolution of metallic ions, this effect was insufficient to totally inhibiting the reaction between the reactive surface of the medium carbon steel and the acidic aggressive environment.

Scanning electron microscopy (SEM). The SEM micrographs of steel in seawater in the absence and presence of 7.5 and 10 mL of bulk and NP solution of *J. curcas* leaf extract are given in Figures 7(a)–7(e). As shown in Figure 7(a), the steel surface was extremely defective without the inhibitors because of metal dissolution in the corrosive solution. The surface was greatly porous, and big and deep holes emerged. Nevertheless, the steel surface's appearance was noticeably distinguished once the inhibitors were added to the corrosive solution. Figures 7(b) and 7(c) show that the dissolution rate of the steel was considerably

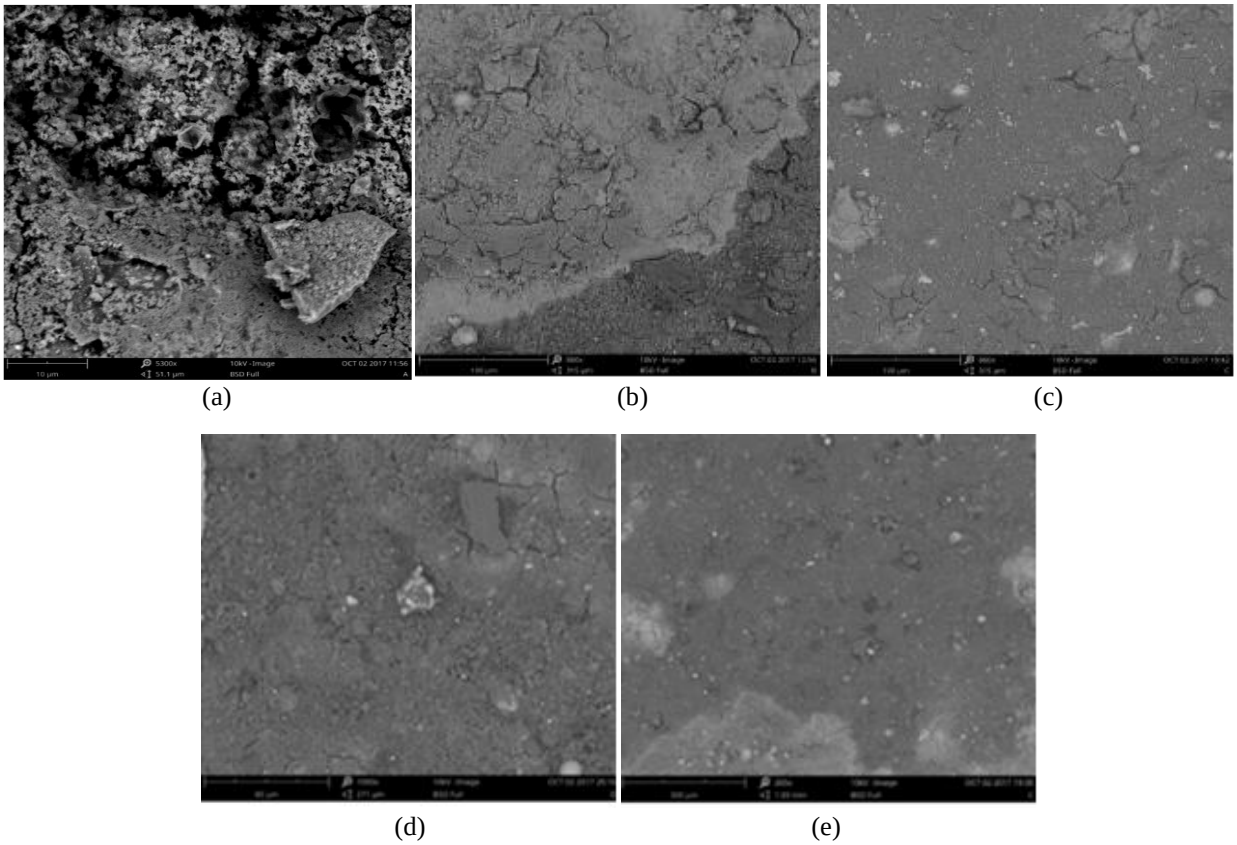

Figure 7. SEM Images of Carbon Steel Immersed in (a) Seawater without the Extract; (b) Seawater with 7.5 mL of Bulk *J. curcas* Extract; (c) Seawater with 10 mL of Bulk *J. curcas* Extract; (d) Seawater with 7.5 mL of Nanoparticle Solution of *J. curcas* Extract; (e) Seawater with 10 mL of Nanoparticle Solution of *J. curcas* Extract

decreased and the damage and roughness were decreased by the protection film formed on the metal surface [34, 35]. A smoother surface appeared in the presence of the NP solution (Figures 7(d) and 7(e)) compared with that after the bulk extract addition (Figures 7(b) and 7(c)). These results revealed the high IE of the NP solution of *J. curcas* leaf extract.

Conclusions

The nanomaterials synthesized from plant extract were investigated for their corrosion inhibition. Based on the outcomes of the analyses, below conclusions could be drawn: UV-vis spectroscopy confirmed the fabrication of AgNPs at 250–400 nm. With the use of *J. curcas* as reducing agent, the solution showed a transformation of color from pale yellow to reddish brown. This phenomenon indicating that AgNP has been successfully formed.XRD revealed that the average crystallite size of the synthesized AgNPs was 36.4 nm. FTIR analysis showed that the NPs were covered with organic residues. The cathodic and anodic current densities (I_{corr}) decreased significantly upon the introduction of *J. curcas* leaf extract (bulk) and its nanostructure with AgNPs (nano) in sea water. These outcomes confirmed that AgNPs could be incorporated into existing inhibitors to further minimize the corrosion rate.

Acknowledgments

The authors would like to acknowledge the Department of Metallurgical and Materials Engineering, Federal University of Technology, Akure, for providing laboratory facilities, and the Department of Chemical Engineering, Afe Babalola University, Ado Ekiti for the laboratory equipment used during this research.

References

[1] Banerjee, P., Satapathy, M., Mukhopahayay, A., Das, P. 2014. Leaf extract mediated green synthesis of silver nanoparticles from widely available Indian plants: synthesis, characterization, antimicrobial property and toxicity analysis. BioResources BioProcessing. 1(1): 1–10, https://doi.org/10.1186/s40643-014-0003-y.

[2] Ajeboriogbon, A.F., Adewuyi, B.O., Talabi, H.K. 2019. Synthesis of silver nanoparticles from selected plants extract. Acta Tech. Corviniensis-Bull. Eng. 12(2): 55–58.

[3] Khan, M., Khan, M., Kuniyil, M., Adil, S.F., Al-Warthan, A., Alkhathlan, H.Z., Tremel, W., Tahir, M.N., Siddiqui, M.R.H. 2014. Biogenic synthesis of palladium nanoparticles using *Pulicaria glutinosa* extract and their catalytic activity towards the Suzuki coupling reaction. Dalton Trans. 43: 9026–9031, https://doi.org/10.1039/c3dt53554a.

[4] Félix-Silva, J., Giordani, R.B., Silva-Jr, A.A.D., Zucolotto, S.M.Z., Fernandes-Pedrosa, M.D.F. 2014. *Jatropha gossypiifolia* L. (Euphorbiaceae): A Review of Traditional Uses, Phytochemistry, Pharmacology, and Toxicology of This Medicinal Plant. Evid.-based Complement. Altern. Med. 2014: 369204, https://doi.org/10.1155/2014/369204.

[5] Omotoyinbo, J.A., Oloruntoba, D.T., Olusegun, S.J. 2013. Corrosion inhibition of pulverized *Jatropha curcas* leaves on medium carbon steel in 0.5 M H_2SO_4 and NaCl environments. Int. J. Sci. Technol. 2(7): 510–514.

[6] Das, R.K., Brar, S.K., Verma, M. 2016. Checking the biocompatibility of plant-derived metallic nanoparticles:Molecular perspectives. Trends Biotechnol. 34(6): 440–449, https://doi.org/10.1016/j.tibtech.2016.02.005.

[7] Thakkar, K.N., Mhatre, S.S., Parikh. R.Y. 2010. Biological synthesis of metallic nanoparticles. Nanomed. Nanotechnol. Biol. Med. 6(2): 257–262, https://doi.org/10.1016/j.nano.2009.07.002.

[8] Shankar, S.S., Rai, A., Ahmad, A., Sastry, M. 2004. Rapid synthesis of Au, Ag, and bimetallic Au core–Ag shell nanoparticles using Neem (*Azadirachta indica*) leaf broth. J. Colloid Interface Sci. 275(2): 496–502, https://doi.org/10.1016/j.jcis.2004.03.003.

[9] Rodríguez-León, E., Iñiguez-Palomares, R., Navarro, R.E., Herrera-Urbina, R., Tánori, J., Iñiguez-Palomares, C., Maldonado, A. 2013. Synthesis of silver nanoparticles using reducing agents obtained from natural sources (*Rumex hymenosepalus extracts*). Nanoscale Res. Lett. 8(1): 1–9, https://doi.org/10.1186/1556-276X-8-318.

[10] Barik, T.K., Sahu, B., Swain, V. 2008. Nanosilica–from medicine to pest control. Parasitol. Res. 103(2): 253–258, https://doi.org/10.1007/s00436-008-0975-7.

[11] Umoren, S.A., Obot, I.B., Gasem, Z.M. 2014. Green synthesis and characterization of silver nanoparticles using red apple (*Malus domestica*) fruit extract at room temperature. J. Mater. Environ. Sci. 5(3): 907–914.

[12] Khan, I., Saeed K., Khan I. 2019. Nanoparticles: Properties, applications and toxicities. Arab. J. Chem. 12(7): 908–931, https://doi.org/10.1016/j.arabjc.2017.05.011.

[13] Mody, Vicky V., Rodney Siwale, Ajay Singh, and Hardik R. Mody. 2010. Introduction to metallic nanoparticles. J. Pharm. Bioallied Sci. 2(4): 282, https://doi.org/10.4103/0975-7406.72127.

[14] Gakiya-Teruya, M., Palomino-Marcelo, L. and Rodriguez-Reyes, J.C.F. 2019. Synthesis of highly concentrated suspensions of silver nanoparticles by two versions of the chemical reduction method. Method. Protoc. 2(1): 3, https://doi.org/10.3390/mps2010003.

[15] Sangeetha, R., Niranjan, P., Dhanalakshmi, N. 2016. Characterization of silver nanoparticles synthesized using the extract of the Leaves of *Tridax procumbens*. Res. J. Med. Plant. 10(2): 159–166.

[16] Moodley, J.S., Krishna, S.B.N., Pillay, K., Govender, P. 2018. Green synthesis of silver nanoparticles from *Moringa oleifera* leaf extracts and its antimicrobial potential. Advances in Natural Sciences: Nanosci. Nanotechnol. 9(1): 015011, https://doi.org/10.1088/2043-6254/aaabb2.

[17] Garibo, D., Borbón-Nuñez, H.A., de León, J.N.D., Mendoza, E.G., Estrada, I., Toledano-Magaña, Y., Tiznado, H., Ovalle-Marroquin, M., Soto-Ramos, A.G., Blanco, A., Rodríguez, J.A. 2020. Green synthesis of silver nanoparticles using *Lysiloma acapulcensis* exhibit high-antimicrobial activity. Sci. Rep. 10: 12805, https://doi.org/10.1038/s41598-020-69606-7.

[18] Mittal, J., Jain, R., Sharma, M.M. 2017. Phytofabrication of silver nanoparticles using aqueous leaf extract of *Xanthium strumerium* L. and their bactericidal efficacy. Adv. Natural Sci. Nanosci. Nanotechnol. 8(2): 025011, https://doi.org/10.1088/2043-6254/aa6879.

[19] Christensen, L., Vivekanandhan, S., Misra, M., Mohanty, A.K. 2011. Biosynthesis of silver nanoparticles using murraya koenigii (curry leaf): an investigation on the effect of broth concentration in reduction mechanism and particle size. Adv. Mat. Lett. 2(6): 429–434, https://doi.org/10.5185/amlett.2 011.4256.

[20] Selvi, B.C.G., Madhavan, J., Santhanam, A. 2016. Cytotoxic effect of silver nanoparticles synthesized from *Padina tetrastromatica* on breast cancer cell line. Adv. Natural Sci. Nanosci. Nanotechnol. 7(3): 035015, https://doi.org/10.1088/2043-6262/7/3/035015.

[21] Ituen, E., Singh, A., Yuanhua, L., Akaranta, O. 2021. Green synthesis and anticorrosion effect of *Allium cepa* peels extract-silver nanoparticles composite in simulated oilfield pickling solution. SN Appl. Sci. 3(6): 1–17, https://doi.org/10.1007/ s42452-021-04670-w.

[22] Ejikeme, C.M., Ezeonu, C.S., Eboatu, A.N. 2014. Determination of physical and phytochemical constituents of some tropical timbers indigenous to Niger Delta area of Nigeria. Eur. Sci. J. 10(18): 247–270.

[23] Talabi, H.K., Adewuyi, B.O., Olaniran, O., Oladele, I.O., Oladotun, J.A. 2022. Microwave accelerated chemical reduction method for the production of copper and copper oxide nanoparticles as nanometal

lubricant additives. J. Chem. Technol. Metall. 57(3): 598–606.

[24] Banerjee, P., Satapathy, M., Mukhopahayay, A., Das, P., 2014. Leaf extract mediated green synthesis of silver nanoparticles from widely available Indian plants: synthesis, characterization, antimicrobial property and toxicity analysis BioResources BioProcessing. 1(1): 1–10, https://doi.org/10.1186/s40643-014-0003-y.

[25] Adewuyi, B.O., Talabi, H.K. 2017. Inhibiting efficiency of locally developed inhibitors (Amaranthusspinosus, Euphorbia heterophylla, Imperatacylindrica and Panicum maximum). Ann. Fac. Eng. Hunedoara. 15(2): 69–76.

[26] Meva, F.E., Segnoua, M.L., Ebonguec, C.O., Ntoumbae, A.A., Kedie, P.B., Delia,V., Etohf, M., Mpondoa, E.M. 2016. Spectroscopic synthetic optimizations monitoring of silver nanoparticles formation from *Megaphrynium macrostachyum* leaf extract. Braz. J. Pharmacog. 26: 640–646, https://doi.org/10.1016/j.bjp.2016.06.002.

[27] Bar, H., Bhui, D.K., Sahoo, G.P., Sarkar, P., Pyne, S., Misra, A. 2009. Green synthesis of silver nanoparticles using seed extract of *Jatropha curcas*. Colloids Surf. A-Physicochem. Eng. Asp. 348(1–3): 212–216, https://doi.org/10.1016/j.colsurfa. 2009.07.021.

[28] Prabu, H.J., Johnson, I. 2015. Plant-mediated biosynthesis and characterization of silver nanoparticles of leaf extracts of *Tragia involucrate, Cymbopogon citronella*, *Solanum verbascifolium* and *Tylophora ovata*. Karbala Int. J. Mod. Sci. 1(4): 237–246, https://doi.org/10.1016/j.kijoms. 2015.12.003.

[29] Narender, B., Ashwani, S., Sanjay, D., Rajesh, P., Viji, V. 2013. Synthesis and optical characteristics of silver nanoparticles on different substrates. Int. Lett. Chem. Phys. Astron. 14: 80–88.

[30] Wagutu, A.W., Yano, K., Sato, K., Park, E., Iso, Y., Isobe, T. 2019. *Musa* AAA and *Jatropha curcas* L. sap mediated TiO_2 nanoparticles: Synthesis and characterization. Sci. Afr. 6: e00203, https://doi.org/10.1016/j.sciaf.2019.e00203.

[31] Naz, M., Nasiri, N., Ikram, M., Nafees, M., Qureshi, M.Z., Ali, S., Tricoli, A. 2017. Eco-friendly biosynthesis, anticancer drug loading and cytotoxic effect of capped Ag-nanoparticles against breast cancer. Appl. Nanosci. 7(8): 793–802, https://doi.org/10.1007/s13204-017-0615-6.

[32] Perveen, R., Shujaat, S., Naz, M., Qureshi, M.Z., Nawaz, S., Shahzad, K., Ikram, M. 2021. Green synthesis of antimicrobial silver nanoparticles with Brassicaceae seeds. Mater. Res. Expr. 8(5): 055007, https://doi.org/10.1088/2053-1591/ac006b.

[33] Logeswari, P., Silambarasan, S., Abraham, J. 2012. Synthesis of silver nanoparticles using plants extract and analysis of their antimicrobial property. J. Saudi Chem. Soc. 19: 311–317, https://doi.org/ 10.1016/j.jscs.2012.04.007.

[34] Aruna, J.K., Jayaraman, A. 2012. Green fabrication of silver nanoparticles by gum Tragacanth (*Astragalus gummifer*): A dual functional reductant and stabilizer. J. Nanomater. 2012: 869765, https://doi.org/10.1155/2012/869765.

[35] Oguzie, E.E. 2007. Corrosion inhibition of aluminium in acidic and alkaline media by *Sansevieria trifasciata* extract. Corros. Sci. 49(3): 1527–1539, https://doi.org/10.1016/j.corsci.2006.08.009.